EG0500268
Thermal Analysis Of The ITER Blanket First Wall

A. A. Badawi*, h. I. Shahbunder†, m. H. Khalil, and m. Morsy
Physics Dept., Science Faculty, Ain Shams University, Cairo, Egypt
Dept. of Nuclear Engineering, Alexandria University, Alexandria,Egypt
alyabadawi@yahoo.com, †hib75@gawab.com

ABSTRACT

The 3D temperature distribution in the First Wall (FW) of the International Thermonuclear Experimental Reactor (ITER) blanket is studied. The effect of FW exposure to different heat fluxes and heat generation rates on the temperature distribution inside the wall is also examined.

The design of FW adopted by ITER council in 2001 is taken as a reference design for the FW through the analysis. The study reveals that the maximum and minimum temperatures increase linearly along the poloidal direction according to the specified incident heat flux and heat generation. The study also indicates a linear variation for the coolant temperature along the cooling channels throughout the poloidal direction.

Key Words: ITER Blanket/ Heat Transfer Analysis/ Blanket First Wall/ Heat Equation.

INTRODUCTION

The function of the ITER blanket system is to provide thermal and nuclear shielding to the vessel and external machine components. The blanket system is also designed to make possible the planned partial conversion of the shielding blanket to the breeding blanket in a later stage of operation [1].

The primary first wall (FW) is the main plasma facing part of the blanket system. It covers a surface of 680 m^2 around the plasma. Its main functions are [1]:

a- to provide a low-Z, low-impurity plasma-compatible surface;

b- to withstand radiation and charged particle flux from the plasma during normal operation;

to provide a suitable protection to the shield from direct contact with the plasma and run-away electrons during off-normal events; and,

c- to provide a first high-dose shield which is removable in hot cell.

FW DESCRIPTION

The basic concept of the blanket system is a modular configuration with a mechanical attachment system. The module configuration consists of a shield body on which a separable first wall (FW) is mounted [1].

Each blanket module supports four FW panels. Each FW panel consists of a 10-mm thick beryllium armor in the form of tiles attached to a 22-mm thick Cu-alloy heat sink plate internally cooled by SS cooling tubes with 10 and 12 mm inner and outer diameters, respectively.

The Cu-alloy plate is attached to a 49-mm thick steel back-plate that has a structural plus shielding function (see Fig. 1) [1].

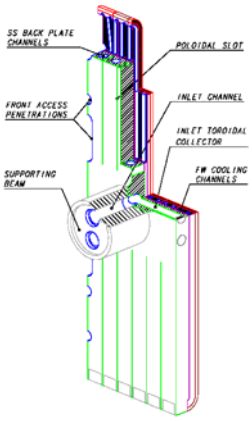

Fig. 1. FW Panel with Central Attachment [1]

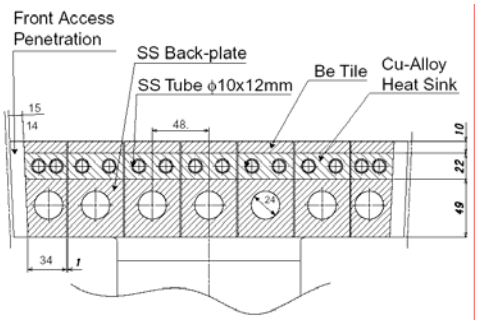

Fig. 2. FW cross-section [1]

A simple straight poloidal cooling channel layout is used in the panel, except for the tubes adjacent to the penetrations, which slightly diverge at their ends in order to provide enough space for their seal welding to the SS back-plate (see Fig. 2). [1]

FW MODEL

A unit cell consisting of one of the semi-symmetric 7 units that form the FW panel is taken as a model where the temperature distribution inside can express the temperatures at the rest of the FW. Fig. 3 shows the unit cell representing the FW. The unit cell includes 3 layers; a 10-mm Be layer, a 22-mm CuCrZr layer, and a 49-mm SS layer. Two SS cooling channels in the Cu layer with inner and outer diameters 10 and 12mm, respectively and single channel in the SS layer with diameter 24mm are included. The cell's cross section is extended in the poloidal direction for 1095 mm.

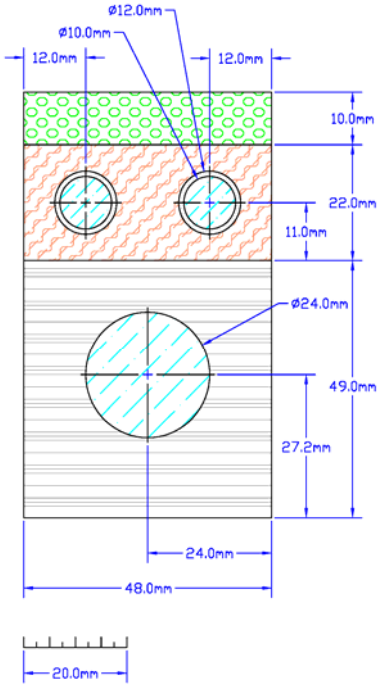

Fig. 3. FW panel model (Unit Cell)

The height in the poloidal direction is then divided in the analysis into 11 sections, each with a 100-mm height, except for the 11th section which is 95 mm. The outlet coolant temperature of each section is considered to be the inlet temperature of the following one.

The heat diffusion equation general form in Cartesian coordinates provides the basic tool for the heat conduction analysis. From its solution, we can obtain the temperature distribution T(x, y, z) as a function of time: [2]

$$\frac{\partial}{\partial x}\left(k\frac{\partial T}{\partial x}\right)+\frac{\partial}{\partial y}\left(k\frac{\partial T}{\partial y}\right)+\frac{\partial}{\partial z}\left(k\frac{\partial T}{\partial z}\right)+\dot{q}=\rho c_p\frac{\partial T}{\partial t} \quad \textbf{(1)}$$

Where T is the temperature (K) at position (x, y, z) and time t (s), k is the thermal conductivity (W/m.K), $\dot{q}$ is the rate of heat generation (W/m^3), ρ and c_p are the material's density (kg/m^3) and specific heat (J/kg.K), respectively.

The heat transferred by conduction through the first wall is removed by convection through the coolant channels. The law governing this process is Newton's law of cooling:

$$q = hA(T_s - T_\infty) \quad \textbf{(2)}$$

where q is the convection heat rate, h is the coefficient of heat transfer (W/m^{2}K), A is the surface area of the pipes, T_s and T_∞ are the temperatures at the surface of the pipe and inside the coolant, respectively.

A numerical solution is used for solving this equation rather than analytical solution due to the complexity of the problem geometry. The numerical technique used is the finite-element method. The two dimensional thermal analysis software called FEHT is used for this purpose.

MODEL CALCULATIONS

Table 1 shows the properties of the materials used inside the blanket at 200 ^{o}C.

Table 1. Blanket materials properties at 200^{o}C. [5]

Material	Density kg/m^3	Thermal conductivity $W \cdot m^{-1}K^{-1}$	Specific heat $J \cdot kg^{-1}K^{-1}$
Be	1840	130	1988
CuCrZr	8900	300	896
SS 316L	7900	16	536

1. Calculation of the coolant mass flow rate

The average total coolant mass flow rate in the module equals the total flow inside all the modules (3,378 kg/s) divided by their numbers (421) = 8.0 kg/s

As each blanket module is divided into 4 equal FW panels, an overall equal share of ¼ of the coolant mass flow rate entering the blanket module is designated for each FW panel. This is equivalent to (8.0/4) kg/s = 2.0 kg/s.

For the FW panel under study, we have 14 SS pipes with inner diameters of 10 mm in the Cu-layer and 7 tubes with diameter ϕ 24 mm drilled inside the SS-layer [1]. The coolant mass flow rate is distributed equally along the narrow and the wide tubes separately according to their cross sectional area. Hence the mass flow rate in each *narrow pipe* = (total mass flow in the FW panel) × (one narrow pipe cross sectional area) / (total cross sectional area of narrow and wide tubes) = 0.037 kg/s.

Similarly, the mass flow rate in each *wide tube* = (total mass flow in the FW panel) × (one wide tube cross sectional area) / (total cross sectional area of narrow and wide tubes) = 0.212 kg/s.

2. Determination of the coolant coefficient of heat transfer

The convection heat transfer coefficient, *h*, can be obtained for fluids in both brands of tubes as:

$$h = \frac{Nu_D k}{D} \quad \textbf{(3)}$$

Where k is the thermal conductivity of the fluid and D is the diameter of the pipe. Nu_D is the Nusselt number, which depends on the type of flow, flow conditions, geometry of the problem and surface conditions of the pipe. A classical expression for computing the Nusselt number for fully developed (hydrodynamically and thermally) turbulent flow in a smooth circular tube is obtained from the *Dittus-Boelter equation*

$$Nu_D = 0.023 \mathrm{Re}_D^{4/5} \mathrm{Pr}^n \quad \textbf{(4)}$$

where n=0.4 for fluid heating, which is our case; and n=0.3 for cooling. The equation above has been confirmed experimentally for the following range of conditions: [2]

i) $0.7 \leq \mathrm{Pr} \leq 160$

ii) $\mathrm{Re_D} \geq 10{,}000$

iii) Tube length/diameter ≥ 10

The Reynolds number, Re_D, is defined as [2]

$$\mathrm{Re}_D = \frac{4\dot{m}}{\pi D \mu} \quad \textbf{(5)}$$

For flow inside a tube, Reynolds number may be used as a criterion for laminar and turbulent flow as follows: [4]

For $\mathrm{Re_D} \leq 2300$, the flow is laminar;

$\mathrm{Re_D} > 2300$, the flow is turbulent.

The Prandtl number, Pr, is defined as [2]

$$\mathrm{Pr} = \frac{\nu}{\alpha} \quad \textbf{(6)}$$

where ν is the kinematic viscosity (m^2/s) and α is the thermal diffusivity (m^2/s).

Note that eq. (4) was used to calculate the Nusselt number after confirming that Re_D showed the water flow in both types of pipes to be turbulent.

A summary of the calculated coolant properties is shown in Table 2.

Table 2. Summary of coolant properties calculated values.

Coolant property	**ϕ10 mm tubes**	**ϕ24 mm tubes**
Inlet temperature °C	100	100
Rate of mass flow, $\dot{m}$ kg/s	0.037	0.212
Reynolds number, $\mathrm{Re_D}$	16,885.3	40,311.6
Nusselt number, $\mathrm{Nu_D}$	69.5	139.4
Convection coefficient, h, W m^{-2} K^{-1}	4,726	3,949.7

3. Heat Flux and Heat Generation

The Bremssthralung, synchrotron and line radiation deposit an average power of 0.25 MW/m^2 on the first wall, with local excursions up to 0.5 MW/m^2 in total. The components are dimensioned to cope with the largest value while the cooling circuit is sized for the average power. [3]

The average neutron flux of 1 MW/m^2, incident on FW surface, induces in the FW material bulk nuclear heating of 16 MW/m^3, which decays exponentially inside the module by about one order of magnitude for every 20 cm, typical 80/20 steel and water mixture, with margin for the geometries discontinuities [3].

Hence, the nuclear heat generation; based on the prior radial dependence, can be formulated mathematically as

$$\dot{q} = ae^{-by} \quad \textbf{(7)}$$

where y is the radial direction, a and b are constants to be determined as follows:

At the surface of the FW, $y = 0$ and the heat generation is maximum, i.e. $\dot{q} = \dot{q}_{max}$ MW/m^2. After a depth of $y = 0.2$ m, the heat generation is reduced by one order of magnitude, i.e. $\dot{q} = (q_{max}/10)$ MW/m^2. Solving eq. (6) for both conditions, we get:

$A = \dot{q}_{max}$ MW/m^2

$b = 11.51$ m^{-1}

Hence $\dot{q}$ can be written on the form

$$\dot{q} = \dot{q}_{max} e^{-11.51y} \quad \textbf{MW/m}^{\textbf{3}} \quad \textbf{(8)}$$

4. Thermal analysis

FEHT software was used in the analysis. The geometry of the problem was entered to the program in centimeters. The toroidal direction is expressed by the x-axis and the radial direction by the y-axis. The FW unit cell shown in Fig. 3 was divided into 7 blocks, as shown in Fig. 4, the coordinates of each block was calculated such that the rectangular blocks have 4 coordinates while the circular blocks (cooling channels boundaries) were divided into 18 segments for each of the upper (2) channels, and 36 segments for the lower channel.

The outlines of the FW unit cell are then drawn in FEHT using the coordinates calculated above (Fig. 4). The heat generation is entered as a function in y-axis, taking into account that FEHT uses cm units. Moreover, the zero of the y-axis will begin from the end of the SS layer, as shown in Fig. 4, so the appropriate form of the heat generation function would be:

$$\dot{q} = \dot{q}_{max} e^{-11.51(8.1-y)/100} \ \textbf{MW/m}^{\textbf{3}} \quad \textbf{(9)}$$

The boundary conditions are then fed for each outline according to type of material, convection coefficient and values of heat flux and heat generation in each case. The model is divided into nodes and element lines manually to form a primary mesh (see Fig. 5).

The mesh is then reduced automatically to the desired density within a specified limit. After reducing the mesh, we have 3898 node, 11196 line segments, and 7296 triangular element equivalent to 3898 unknown temperature at each FW layer.

The model was used to study cases with different heat flux and generation. The inlet temperature in all the cases is constant at 100^{o}C. The coolant mass flow rate is also held constant at the values calculated before.

The heat flux incident on the 3 other surfaces (all except the Be-layer surface) of the FW unit model is assumed to be zero due to symmetry for the right and left sides and for assuming a thermal insulation (instead of a shield block) at the lower side of the FW (bottom of the SS layer).

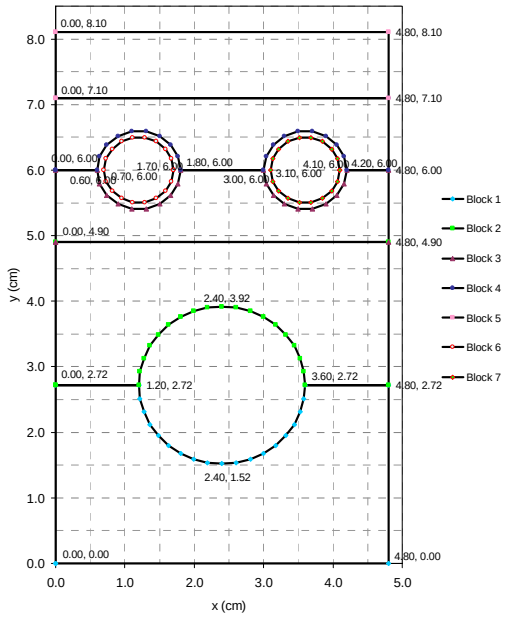

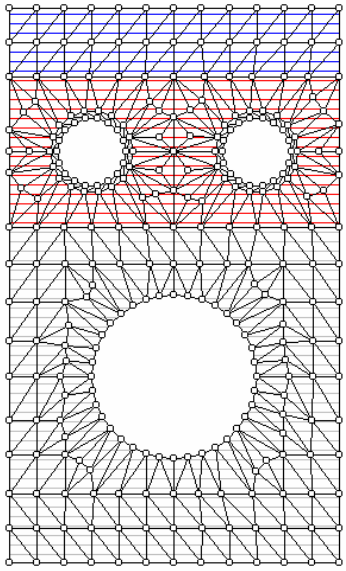

Fig. 4. FW unit model blocks coordinates. **Fig. 5. Manual FW mesh using FEHT (289 node)**

After the 2D analysis is done, the amount of heat flow rate per poloidal unit length (W/m), *q*, to the cooling channels is determined. This amount is used to calculate the value of outlet temperature from the section considered, using the following equation:

$$l\,q = \dot{m}\,c\,(T_{out} - T_{in}) \qquad (10)$$

Where *l* is the height of the section (m), $\dot{m}$ is the coolant mass flow rate (kg/s) and *c* is its specific heat (J/kg.K). Later, the value of T_{out} is fed to the following section as its coolant T_{in} and the process is repeated until the *z* or *poloidal* FW height (1095 mm) is finished.

An example of the thermal analysis output is shown in Fig. 6. This figure represents a case with heat flux of 0.125 MW/m^2 and a $\dot{q}_{max}$ of 8 MW/m^3, for the first section (from z = 0 to 0.1 m). Each shaded band represents a certain range of temperature which varies according to the shown gray scale value in the figure. A full detail of temperature values along each node (for the 3898 nodes) can be given in a tabular output versus the node coordinates (x, y).

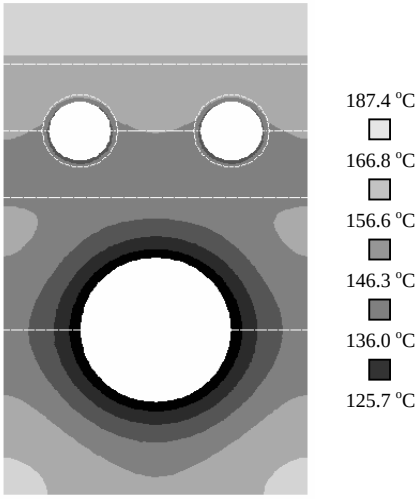

Fig. 6. FW unit model temperature contours for a case with 0.125 MW/m^2 heat flux and 8 MW/m^3 maximum heat generation.

RESULTS AND DISCUSSION

Nine cases of different heat flux and generation were studied. The values of the chosen flux and maximum generation are varied around the average values estimated by the design reference [1]. The considered cases are shown in Table 3.

Table 3. Selected cases for study

Case #	Heat Flux MW/m^2	Max. Heat Gen. MW/m^3
1	0.125	0
2	0.125	8
3	0.125	15
4	0.2	15
5	0.25	15
6	0.25	16
7	0.5	0
8	0.5	8
9	0.5	16

Fig. 7 shows the variation of the minimum and maximum temperatures and the coolant temperature in both types of pipes, along the poloidal direction (z-direction). The results in the figure are for case#2. The change in the coolant temperature in the poloidal direction is found to be linear. This can be explained by eq. (10), which shows that the temperature change in the coolant pipes is linear with the rate of heat transferred to the pipes.

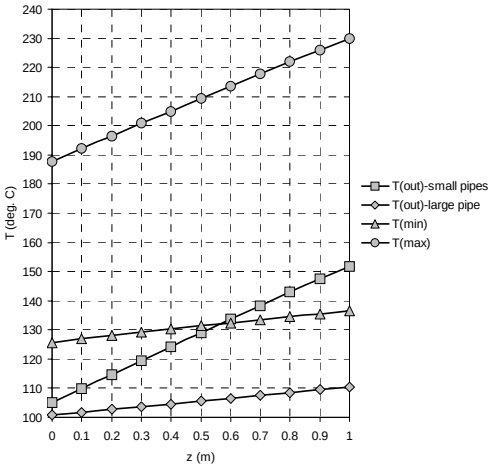

Fig. 7. Variation of the minimum and maximum temperature and the coolant temperature along the poloidal direction for case#2.

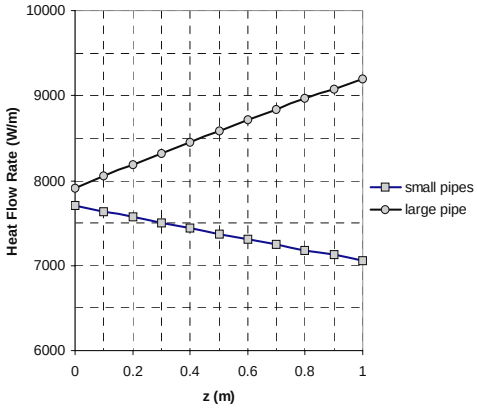

Fig. 8. The variation of the rate of heat transferred to the small and large pipes along the poloidal direction for case#2.

The maximum and minimum temperatures are found to increase along the z direction. Note that since the temperature of the coolant increases along z, the temperature of the FW must increase in order to remove the same amount of heat from each layer.

Fig. 8 shows the rate of heat transferred to the small and large coolant channels along the poloidal direction. Note that the summation of the heat transfer in both types is constant in each layer and is equal to the sum of the incident heat flux and the heat generation.

It can be seen from the figure that in the beginning the heat is divided almost equally between the two types. This is to be expected since the water enters in both types with the same inlet temperature. However as the coolant flows through the channels the temperature in the smaller tubes becomes higher than that in the large tube. Two factors contribute to this: the first is that the small pipes are

located closer to the surface of the beryllium, where the heat flux is incident. The second factor is that the mass flow in the small pipes is less than that in the large pipe. This makes the temperature of the small pipes rise more rapidly than the large pipe. The result would be that more heat will go through the large channel as *z* increases.

The temperature variation along the poloidal direction was found to depend on the heat generation and flux. However the same behavior as in Figs. 7 and 8 was seen in all cases.

Table 4 shows, for each of the nine cases considered (see Table 3), the maximum and minimum temperatures, which are always located in the top and bottom layers, respectively, and the exit coolant temperature in both types of pipes.

Table 4. Different temperatures calculated in each case.

Case#	Min. Temp. ^{o}C	Max. Temp. ^{o}C	Exit Coolant Temp. ^{o}C (small pipes)	Exit Coolant Temp. ^{o}C (large pipes)
1	100.4	137.0	117.3	101.3
2	125.7	230.0	151.8	110.5
3	145.2	299.2	182.0	118.5
4	147.6	329.8	192.3	119.3
5	148.5	350.1	199.3	119.8
6	151.5	359.3	203.6	121.0
7	101.7	304.0	169.2	105.3
8	127.7	383.0	203.7	114.4
9	153.7	462.0	238.1	123.6

Table 4 shows that the minimum temperature is affected by the heat generation and not by the heat flux. This is better illustrated in Figs. 9 and 10.

In Fig. 9 the maximum and minimum temperatures are plotted versus the heat flux incident on the beryllium surface for a constant maximum heat generation of 15 MW/m^3. The figure clearly shows that the change in the minimum temperature is negligible. Changing the heat flux by 400% changes the temperature by about 6%.

The maximum temperature however is seen to be dependent on the heat flux. Changing the heat flux from 0.125 MW/m^2 to 0.2 MW/m^2 (60% increase) increases the maximum temperature from 299.2^{o}C to 329.8^{o}C (10%). Increasing the heat flux from 0.25 MW/m^2 to 0.5 MW/m^2 (100% increase) increases the maximum temperature from 350.1^{o}C to 462.0^{o}C (32%).

The fact that T_{max} depends on the heat flux whereas T_{min} doesn't can be explained by noting the place of each temperature. T_{max} is always located on the beryllium surface facing the incident heat flux. T_{min} is found in the back of the first wall. Thus most of the incident heat flux will have been removed by the coolant before reaching that position.

Fig. 10 shows the effect of the heat generation (represented by the maximum rate of heat generation, $\dot{q}_{max}$) for a constant heat flux of 0.5 MW/m^2. Changing $\dot{q}_{max}$ from 8 MW/m^3 to 16 MW/m^3 (100% increase) changes T_{min} from 127.7 ^{o}C to 153.7 ^{o}C (20% increase), and changes T_{max} from 383.0 ^{o}C to 462.0 ^{o}C (20% increase).

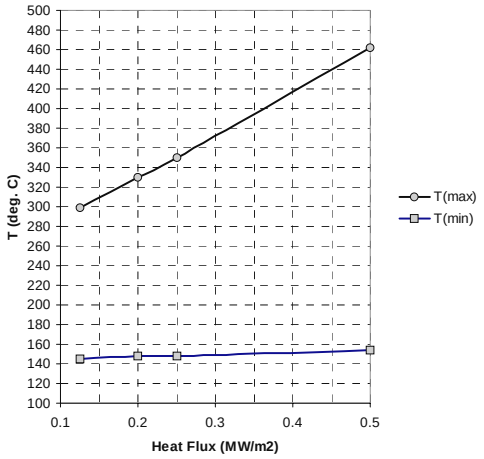

Fig. 9. Effect of the heat flux on the minimum and maximum temperatures inside the FW for a constant maximum heat generation.

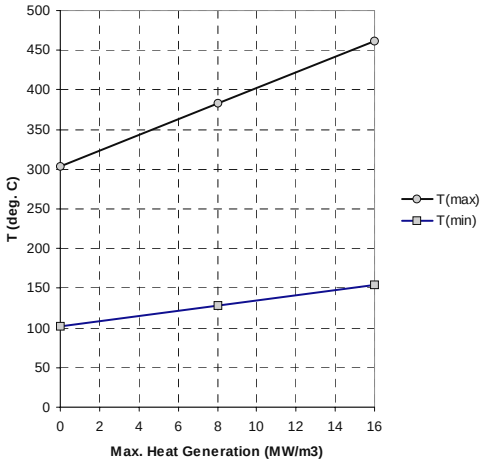

Fig. 10. Effect of the heat generation on the minimum and maximum temperatures inside the FW for a constant heat flux.

Fig. 11 shows the effect of the heat flux on the coolant exit temperatures of both the small and large pipes. The heat flux is seen to have a negligible effect on the exit temperature of the coolant in the large channel. Again this is because of its location at the back of the FW, far from the surface exposed to the heat flux. The exit temperature of the coolant in the small pipes, however, is seen to depend on the heat flux. Changing the flux from 0.25 to 0.5 (100% increase) changes the temperature from 199.3 ^{o}C to 238.1 ^{o}C (20% increase). This dependence is due to the fact that the small pipes remove a large fraction of the incident heat flux.

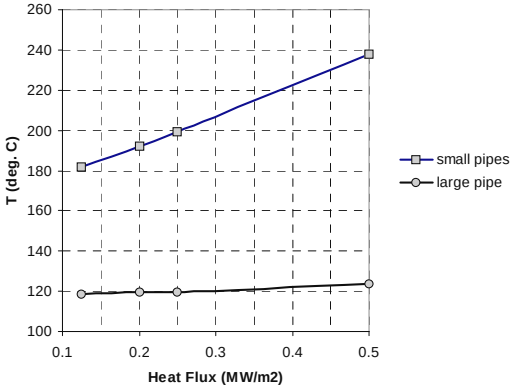

Fig. 11. Effect of the incident heat flux on the coolant exit temperature for a constant maximum heat generation.

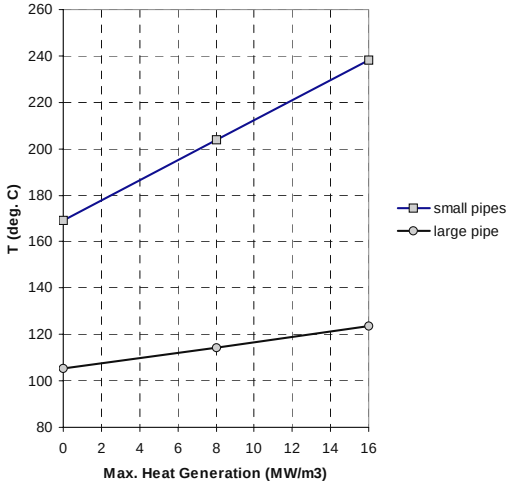

Fig. 12. Effect of the heat generation on coolant exit temperature for a constant heat flux.

Fig. 12 shows the effect of the heat generation on the exit temperatures of the coolant in both the small and large pipes. Here the heat generation affects the coolant temperature in both types. Changing $\dot{q}_{\max}$ from 8 MW/m^3 to 16 MW/m^3 (100% increase) changes the temperature of the small pipes from 203.3 ^{o}C to 238.1^{o}C (17% increase), and of the large pipe from 114.4 ^{o}C to 123.6 ^{o}C (7% increase). This dependence is because both pipes remove the heat generation.

However the change in the temperature of the large pipe is less than that in the small pipe. This is due to its larger mass flow rate and also because there is less heat generation around the large pipe.

CONCLUSION

The temperature distribution in the first wall of the ITER blanket was studied. The effect of FW exposure to different thermal fluxes and rates of heat generation on the temperature distribution inside the wall was examined.

A model has developed to describe the thermal behavior inside a unit cell representing the first wall. The model was used to determine the temperature distribution inside the FW and in the coolant channels. The following conclusions were made:

1- The change in the coolant temperature in the poloidal direction is found to be linear.

2- The minimum temperature is always found in the bottom of the first wall, at the back of the stainless steel.

3- The maximum temperature is always found at the top of the first wall, on the beryllium surface facing the incident heat flux.

4- The maximum temperature is found to depend on both the heat flux and the rate of heat generation.

5- The minimum temperature is found to depend only on the rate of heat generation.

6- The coolant exit temperature in the small pipes depends on both the heat flux and the rate of heat generation.

7- The coolant exit temperature in the large channel depends on the rate of heat generation and not on the heat flux.

REFERENCES

(1) "Technical Basis for the ITER Final Design Report (FDR), Plant Description Document", IAEA / ITER EDA DOCUMENTATION SERIES, 2001.

(2) "Introduction to Heat Transfer" 4th Edition, Frank P. Incropera, David P. DeWitt, John Wiley & Sons Inc., 2002.

(3) "Engineering Design of the ITER Blanket and Relevant R&D Results", F. Elio, K. Ioki, P. Barabaschi, L. Bruno, A. Cardella, M. Hechler, T. Kodama, A. Lodato, D. Loesser, D. Lousteau, N. Miki, K. Mohri, R. Parker, R. Raffray, D. Williamson, M. Yamada, W. Daenner, R. Mattas, Y. Strebkov, H. Takatsu. Invited Paper to the 20th SOFT, Marseille, 7-11 September 1998.

(4) "Heat Transfer" 5th Edition, J. P. Holman, McGraw-Hill Inc., 1981.

(5) Private communication with Dr. Filippo Elio, ITER JCT Garching, Max Plack Institute fuer Plasmaphysic, Germany, 2003.